

Ferrimagnetic copper chloride hydroxide

This article has been downloaded from IOPscience. Please scroll down to see the full text article.

2003 J. Phys.: Condens. Matter 15 5629

(<http://iopscience.iop.org/0953-8984/15/32/322>)

View [the table of contents for this issue](#), or go to the [journal homepage](#) for more

Download details:

IP Address: 171.66.16.125

The article was downloaded on 19/05/2010 at 15:02

Please note that [terms and conditions apply](#).

Ferrimagnetic copper chloride hydroxide

S G Yang, T Li, B L Xu and Y W Du

National Laboratory of Solid State Microstructures, Nanjing University, Nanjing 210093, China

E-mail: sgyang@nju.edu.cn

Received 18 May 2003

Published 1 August 2003

Online at stacks.iop.org/JPhysCM/15/5629

Abstract

Magnetic properties of copper chloride hydroxide were studied by using a superconducting quantum interference device. The coercivity of this material was more than 10 000 Oe at 2 K, which is the highest observed in the copper compounds. The magnetic susceptibility as a function of temperature revealed ferrimagnetism in the sample.

Organic magnetism is a topic that has become interesting in recent years [1]. Scientists have paid a great deal of attention to the magnetism of copper in the organic magnets. Pure copper is a kind of diamagnetic material, whose magnetization direction is opposite to that of the applied magnetic field [2, 3]. Antiferromagnetism in cuprate high- T_c superconductors has been widely studied [4, 5]. Some information on the ferromagnetic and antiferromagnetic coupling between copper atoms has been obtained for some copper–organic hybrid composites [6–9]. Here we present the discovery of ferrimagnetism in the copper chloride hydroxide $\text{Cu}_2\text{Cl}(\text{OH})_3$. The Curie temperature is 6.4 K and the coercive field is 10 400 Oe at 2 K, which is believed to be the largest in copper compounds.

The sample was prepared following the techniques of Sharkey [10]. Copper chloride 2-hydrate ($\text{CuCl}_2 \cdot 2\text{H}_2\text{O}$, purity 99%) and sodium hydroxide (NaOH, purity 99%) were used as the starting materials. NaOH aqueous solution (0.03 mol l^{-1}) and $\text{CuCl}_2 \cdot 2\text{H}_2\text{O}$ aqueous solution (0.02 mol l^{-1}) were prepared as reactants. With magnetic stirring, the NaOH solution was added drop-wise into the $\text{CuCl}_2 \cdot 2\text{H}_2\text{O}$ aqueous solution, in which $\text{pH} < 7.6$, at room temperature. The copper chloride hydroxide was precipitated from solution and distilled with de-ionized water. After the water was removed in a dry box, a blue powder sample was obtained. Its structure was examined using a conventional powder x-ray diffraction (XRD) machine with a graphite monochromator (D/max-r C). X-ray intensity data were collected with Cu $K\alpha$ radiation over a 2θ scan from 10° to 60° in steps of 0.02° .

Figure 1 shows a typical XRD pattern for $\text{Cu}_2\text{Cl}(\text{OH})_3$ at room temperature. The intensity peaks can be indexed assuming a rhombohedral unit cell with $a = 13.654 \text{ \AA}$, $c = 14.041 \text{ \AA}$, $Z = 24$, which has been determined as that of paratacamite [11]. Figure 2 shows the crystal structure of paratacamite with space group $R\bar{3}$. In a unit cell, three quarters of the copper

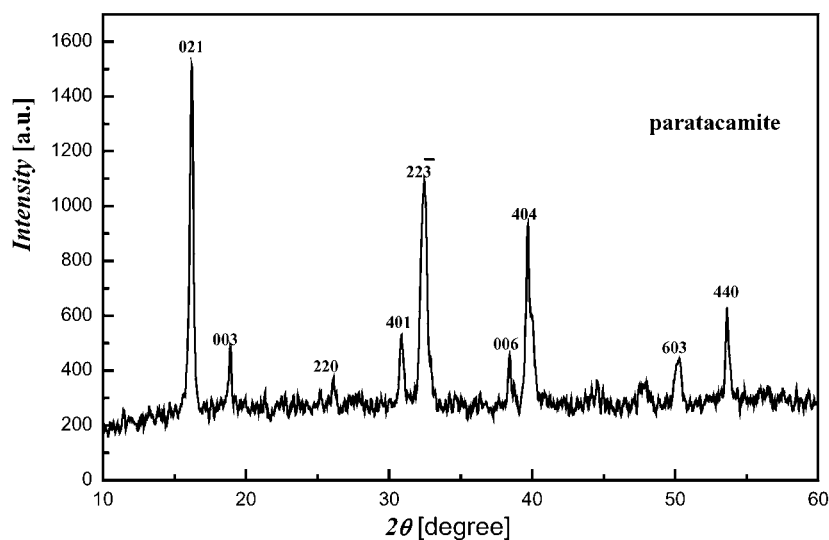


Figure 1. The XRD pattern of the sample.

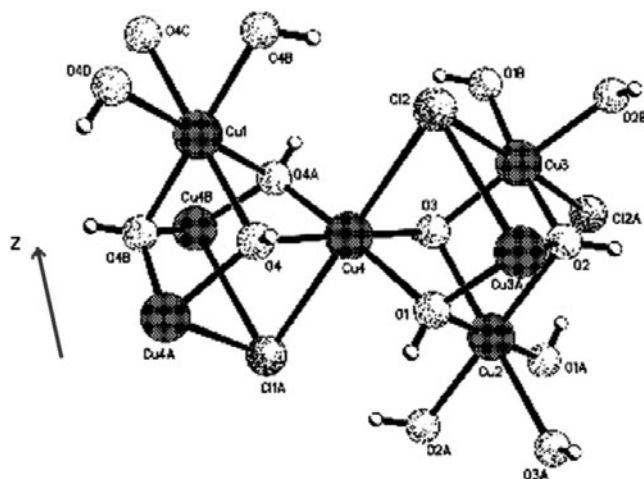


Figure 2. The crystal structure of paratacamite.

atoms are coordinated to four neighbouring O atoms and two distant Cl atoms, giving the expected (4+2) configuration (Cu3 and Cu4), three sixteenths of the copper atoms have (2+4) configurations (Cu2), with two O atoms at 1.93 Å and four O atoms at 2.19 Å, and one sixteenth of the copper atoms have six equivalent O atoms at 2.12 Å (Cu1), as shown in figure 2. Three quarters of the copper atoms (Cu3 and Cu4) form layers and one quarter of the copper atoms (Cu1 and Cu2) are inserted in these layers, constructing a three-dimensional network with OH (or Cl) as bridges. A projective image of the copper atoms along the *z*-direction is shown in figure 3.

In order to exclude effects of impurities, high-purity materials have been used. The impurities in the sample have been determined using inductively coupled plasma analysis (ICP, J-A1100). The impurity concentration is shown in table 1. Only some non-magnetic

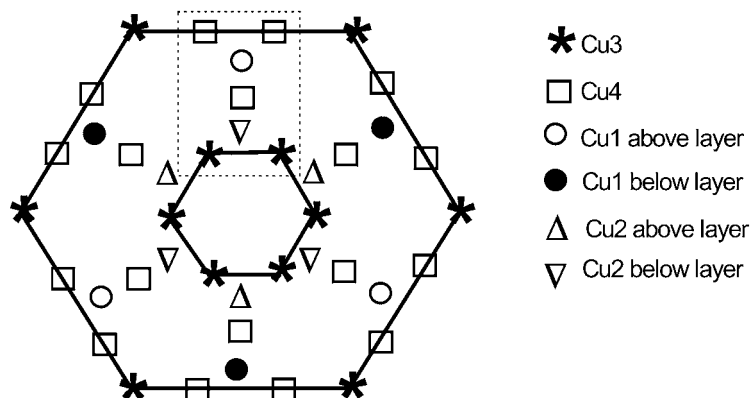


Figure 3. A projective image of copper atoms along the z -direction.

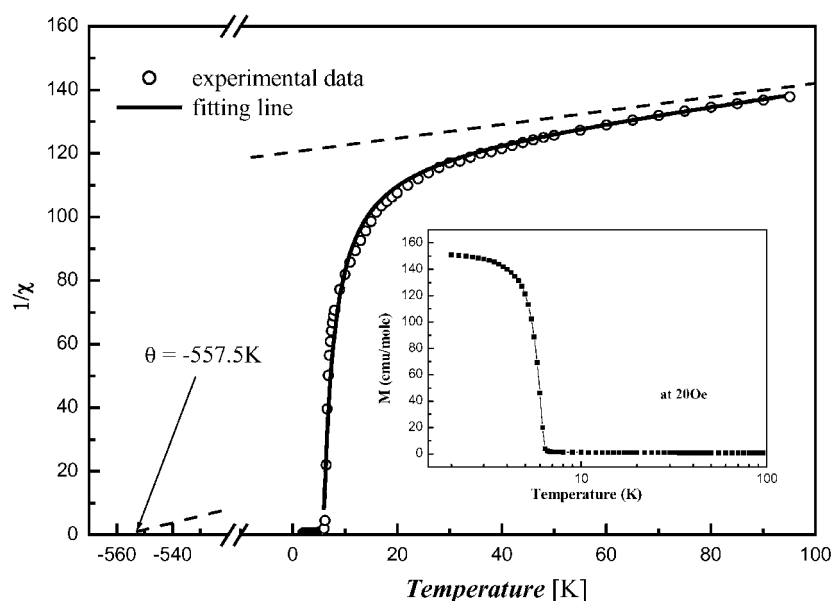


Figure 4. The $1/\chi-T$ curve for the sample in a field of 20 Oe, with the magnetization shown as an inset. ■: magnetization data; ○: $1/\chi$ data; solid line: fitting curve; dashed line: the extension of the linear part of $1/\chi$ to high temperature.

Table 1. The impurity concentration in the sample.

Elemental	Al	Ba	Ca	Cd	Co	Cr	Na	Zn	Mg
Proportion (%)	None	None	None	None	0.002	0.015	None	None	0.04

elements (Cr and Mg) and trace amounts of a magnetic element (Co) can be found, which may make no contribution to the magnetic response of the sample.

Magnetic measurements were performed with a superconducting quantum device (SQUID, MPMS-5S). Figure 4 shows the reciprocal of the magnetic susceptibility ($1/\chi$) of the sample as a function of temperature at 20 Oe. The Curie temperature is confirmed to be

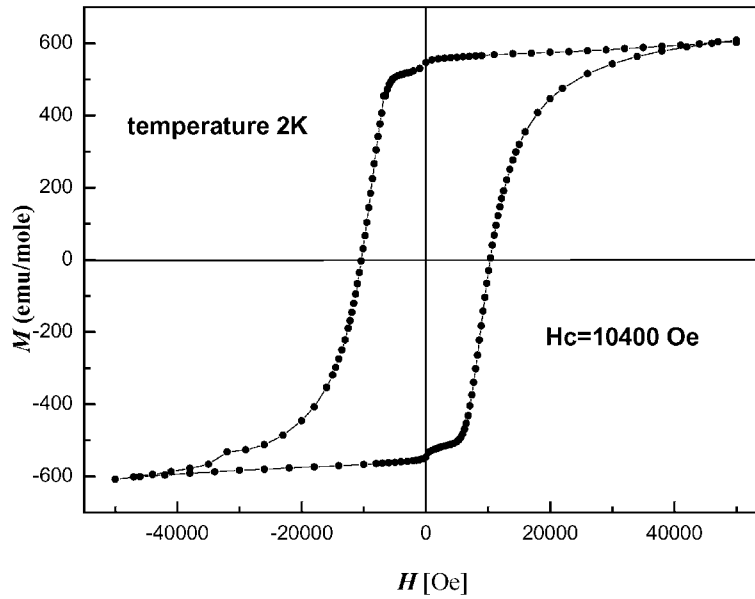


Figure 5. The hysteresis loop of the sample at 2 K.

about 6.4 K. At temperature below 6.4 K, the magnetization saturated to a constant value, as shown in the inset of figure 4.

The saturation magnetization at 2 K is $M_s = 594.17 \text{ emu mol}^{-1}$. The valence is +2 for copper cations in $\text{Cu}_2\text{Cl}(\text{OH})_3$. There are nine electrons, one electron less than in a complete shell, in the 3d shell of every copper ion. Because of the quenching of the angular momentum in the crystal field, the magnetic moment of this material arises mainly from the electron spin [12]. As $s = 1/2$, $g_s = 2$; we thus get the magnetic moment of each Cu^{2+} , which is

$$\mu = g_s \sqrt{s(s+1)} \mu_B = 1.732 \mu_B$$

where the Bohr magneton

$$\mu_B = 9.27 \times 10^{-24} \text{ J T}^{-1}.$$

If all the copper spins aligned in the same direction, the saturation magnetization would be $M_s = 1.935 \times 10^4 \text{ emu mol}^{-1}$, which is much larger than our result. Ferrimagnetism can be regarded as a special kind of antiferromagnetism whose magnetic moments are not totally counteracted. According to molecular field theory [13], the relationship between magnetic susceptibility and temperature beyond the Curie temperature can be described as

$$\frac{1}{\chi} = \frac{T - \theta}{C} - \frac{\zeta}{T - \theta'}.$$

In magnetism, θ and ζ are used to classify magnetic materials. For θ larger than zero and ζ equal to zero, you have ferromagnetism; for θ smaller than zero and ζ equal to zero, you have antiferromagnetism; for θ smaller than zero and ζ larger than zero, you have ferrimagnetism. As regards our sample, by data fitting, we get the Curie constant $C = 4.629 \text{ K}$, Weiss temperature $\theta = -557.5 \text{ K}$, $\theta' = 3.850 \text{ K}$, and $\zeta = 243.5 \text{ K}$. The open circles in figure 4 show experimental data and the line is the fitting curve. The Weiss temperature θ is far below 0 K and ζ larger than zero, indicating the existence of ferrimagnetism in the sample.

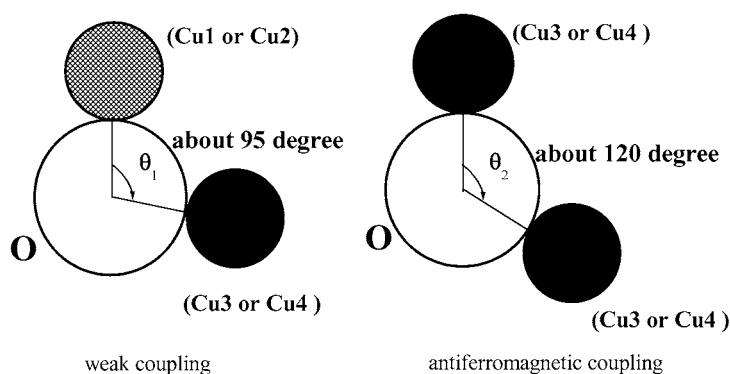


Figure 6. Two kinds of Cu–O–Cu bridge.

Figure 5 shows the magnetic moment as a function of applied field at 2 K. There is a slight discontinuity in M close to $H = 0$. This experimental result may be reflecting the complex magnetic structure of the material. From the hysteresis loop, a coercive field, defined as that where $M = 0$, of 10 400 Oe was obtained. So large a value of the coercive field has not been reported previously for copper compounds.

One possibility is that this ferrimagnetism is arising from a superexchange interaction between copper atoms [14]. The magnetic interaction between copper atoms is mainly affected by the bond lengths and angles [15]. According to superexchange interaction theory: the longer the bond length, the weaker the magnetic interaction between copper atoms; the smaller the bond angle, the weaker the antiferromagnetic interaction between copper atoms. As the bond lengths of Cu–Cl (about 2.7–2.8 Å) are much larger than those of Cu–O (about 1.9–2.2 Å) [10], the superexchange between copper atoms with Cl bridges can be neglected.

From table 2, we see that there are two typical Cu–O–Cu bond angles: one is about 120°, and the other is about 95°. The bond angles between the inserted copper atoms (Cu1 or Cu2) and the layer copper atoms (Cu3 or Cu4) are about 95°, while those between layer copper atoms (Cu3 and Cu4) are about 120° (see figure 6). From Anderson–Kanamori–Goodenough rules [16], weak angle-independent ferromagnetic coupling and strong antiferromagnetic coupling cooperate with each other and lead to a trend in the magnetic coupling: from zero for 90° to the maximum for 180°. A theoretical study of several cuprates showed that the sum of the magnetic couplings tends to zero when the bond angle is about 95° [17].

In the layers, the copper atoms arrange in triangular arrays. The Cu–O–Cu bond angles are about 120°, which leads to antiferromagnetic coupling between copper atoms. There are two kinds of situation for copper atoms (Cu3 and Cu4); their ambient conditions are a little different (figure 7 shows a typical example). Because of the triangle arrangement, the copper spins cannot be totally antiparallel; they should form a 60° triangular magnetic structure. The different situations for the Cu3 and Cu4 may cause a deviation, and thus a net magnetic moment may be left. This is a possibility for the origin of the ferrimagnetism in our sample.

In conclusion, ferrimagnetism is realized in copper chloride hydroxide with a Curie temperature of 6.4 K. The coercive field at the temperature of 2 K is about 10 400 Oe.

Acknowledgments

This work was supported by the Natural Science Fund of Jiangsu Province (BK2001404) and the Key Project for Fundamental Research of China (G1999064508). The authors sincerely

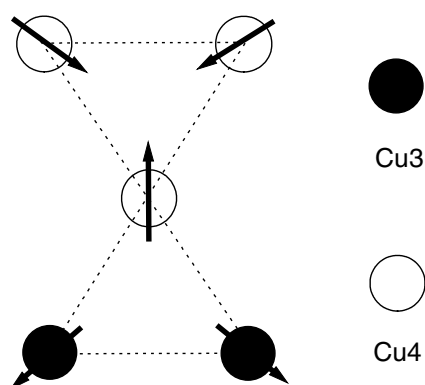


Figure 7. A sketch of the antiferromagnetic coupling between the copper atoms in the layers.

Table 2. Bond lengths and bond angles for Cu–O–Cu.

Cu atom	Bond length (Å)	O atom	Bond length (Å)	Cu atom	Bond angle (deg)
Cu2	1.933	O1	1.969	Cu3	101.37
Cu2	1.933	O1	2.067	Cu4	99.86
Cu3	1.969	O1	2.067	Cu4	114.63
Cu3	1.982	O2	1.999	Cu3	119.52
Cu3	1.982	O2	2.186	Cu2	92.71
Cu3	1.999	O2	2.186	Cu2	95.48
Cu3	1.934	O3	1.986	Cu4	119.77
Cu3	1.934	O3	2.204	Cu2	96.84
Cu4	1.986	O3	2.204	Cu2	93.79
Cu4	1.935	O4	1.990	Cu4	121.91
Cu4	1.935	O4	2.121	Cu1	97.78
Cu4	1.990	O4	2.121	Cu1	96.09

thank Dr K Liu for the magnetic measurement of the samples, Professor D Y Xing for discussion and Dr Samuel Lo for the crystal structure analysis.

References

- [1] Miller J S 2002 *Adv. Mater.* **14** 1105
- [2] Van Vleck J H 1957 *Nuovo Cimento (Suppl.)* **6** 1101
- [3] Morrish A H 1965 *The Physical Principles of Magnetism* (New York: Wiley)
- [4] Mitrovic V F, Sigmund E E, Eschrig M, Bachman H N, Halperin W P, Reyes A P, Kuhns P and Moulton W G 2001 *Nature* **413** 501
- [5] Schon J H, Dorget M, Beuran F C, Xu X Z, Arushanov E, Lagues M and Cavellin C D 2001 *Science* **293** 2430
- [6] Maji T K, Mukherjee P S, Mostafa G, Mallah T, Cano-Boquera J and Chaudhuri N R 2001 *Chem. Commun.* 1012
- [7] Willett R D, Landee C P, Gaura R M, Swank D D, Groenendijk H A and Van Duyneveldt A J 1980 *J. Magn. Magn. Mater.* **15–18** 1055
- [8] Xu Z Q, Thompson L K and Miller D O 2001 *Chem. Commun.* 1170
- [9] Fujita W, Awaga K and Yokoyama T 1999 *Appl. Clay Sci.* **15** 281
- [10] Sharkey J B *et al* 1971 *Am. Mineral.* **56** 179
- [11] Fleet M E 1975 *Acta Crystallogr. B* **31** 183
- [12] Cralin R L 1986 *Magnetochemistry* (Berlin: Springer)

-
- [13] Smart J S 1958 *Phys. Rev.* **101** 585
 - [14] Smit J and Wijn H P J 1959 *Ferrites* (Eindhoven: Philips)
 - [15] Mizuno Y, Tohyama T and Machawa S 1998 *Phys. Rev. B* **58** R14713
 - [16] Anderson P W 1963 *Magnetism* vol 1, ed G T Rado and H Suhl (New York: Academic) p 67
 - [17] Mizuno Y, Tohyama T, Machawa S, Osafune T, Motoyama M, Eisaki H and Uchida S 1998 *Phys. Rev. B* **57** 5326